

Gravitational waves from breaking of an extra $U(1)$ in $SO(10)$ grand unification

Nobuchika Okada*

*Department of Physics and Astronomy,
University of Alabama, Tuscaloosa, Alabama 35487, USA*

Osamu Seto†

*Institute for the Advancement of Higher Education,
Hokkaido University, Sapporo 060-0817, Japan and
Department of Physics, Hokkaido University, Sapporo 060-0810, Japan*

Hikaru Uchida‡

Department of Physics, Hokkaido University, Sapporo 060-0810, Japan

Abstract

In a class of gauged $U(1)$ extended Standard Models (SMs), the breaking of the $U(1)$ symmetry is not only a source for Majorana masses of right-handed (RH) neutrinos crucial for the seesaw mechanism, but also a source of stochastic gravitational wave (GW) background. Such $U(1)$ extended models are well-motivated from the viewpoint of grand unification. In this paper, we discuss a successful ultraviolet completion of a $U(1)$ extended SM by an $SO(10)$ grand unified model through an intermediate step of $SU(5) \times U(1)$ unification. With a parameter set that is compatible with the $SO(10)$ grand unification, we find that a first-order phase transition associated with the $U(1)$ symmetry breaking can be strong enough to generate GWs with a detectable size of amplitude. We also find that the resultant GW amplitude reduces and its peak frequency becomes higher as the RH neutrino masses increase.

*Electronic address: okadan@ua.edu

†Electronic address: seto@particle.sci.hokudai.ac.jp

‡Electronic address: h-uchida@particle.sci.hokudai.ac.jp

I. INTRODUCTION

An extra $U(1)$ gauge interaction is one of promising and interesting extensions of the standard model (SM) of particle physics. Since tiny but non-vanishing neutrino masses are a clear evidence for the existence of the beyond the SM, one of the simplest and the most interesting models is the one based on the gauge group $SU(3)_C \times SU(2)_L \times U(1)_Y \times U(1)_{B-L}$ [1–4], where the additional interaction is from the gauged $U(1)_{B-L}$ (baryon number minus lepton number) symmetry. In the standard $U(1)_{B-L}$ charge assignment, three right-handed (RH) neutrinos have to be introduced to fulfill the gauge and gravitational anomaly cancellation conditions. After Majorana masses of RH neutrinos are generated by the spontaneous $U(1)_{B-L}$ gauge symmetry breaking at a high energy scale, the observed tiny neutrino masses are naturally explained by the so-called seesaw mechanism with the heavy Majorana RH neutrinos through their Yukawa interactions with the SM left-handed neutrinos [5–8]. In addition, one of the three RH neutrinos can be a candidate for the dark matter in our universe [9–14].

Although it is very difficult for any collider experiments to test an additional gauge symmetry if it is broken at very high energies, the detection of a gravitational wave (GW) can be a probe for such an extra $U(1)$ symmetry breaking [15–24]. This is because the first-order phase transition in the early universe is one of the promising sources of stochastic GW background [25–27]. If a first-order phase transition occurred in the early universe, the dynamics of bubble collision [28–32] followed by turbulence of the plasma [33–37] and sonic waves [38–40] had generated GWs, which can be detected by the future experiments, such as Big Bang Observer (BBO) [41], DECI-hertz Interferometer Observatory (DECIGO) [42], Advanced LIGO (aLIGO) [43], and Einstein Telescope (ET) [44].

In this paper, we consider an ultraviolet (UV) completion of such an extra $U(1)$ extended SM. A primary candidate scenario for the completion is the Grand Unified Theory (GUT), in which all the SM gauge interactions are unified into a single gauge interaction at a high energy scale. In this paper, we consider an $SO(10)$ GUT model, in which the extra $U(1)$ gauge group along with the SM gauge group is embedded, and all the SM fermions and RH neutrinos in each generation are also unified into a single **16** representation of $SO(10)$ [45]. Among several possible paths of symmetry breaking from the $SO(10)$ to the SM gauge group, we consider the following: First, $SO(10)$ breaks to $SU(5) \times U(1)$ at a very high

scale $M_{SO(10)}$. Next, the $SU(5)$ breaks to the SM gauge group at a scale $M_{SU(5)} \simeq 10^{16}$ GeV. The extra $U(1)$ is essentially the gauged $B - L$ symmetry and its breaking can take place at any scale below $M_{SO(10)}$. If the extra $U(1)$ symmetry breaking scale is very high, cosmic strings can be the dominant source for stochastic GWs [46–49]. Another promising GW source is the first-order phase transition in the early universe associated with the $U(1)$ symmetry breaking at a scale lower than about 10^7 GeV [50–52]. In previous work on the $U(1)$ extended SMs [19, 23], we have treated the $U(1)$ gauge coupling as a free parameter and have shown that with its suitable choice the first-order phase transition can generate the GWs large enough to be tested in the future experiments. However, once we consider the UV completion by the $SO(10)$ GUT, the $U(1)$ gauge coupling is no longer a free parameter and its low energy value is determined by the condition of the gauge coupling unification. In this paper, we will examine whether the parameter set compatible with the $SO(10)$ unification can generate a detectable size of the GW spectrum.¹

This paper is organized as follows: In the next section, we describe the outline for the $SO(10)$ unification of the $U(1)$ extended SM based on the gauge group of $SU(3)_C \times SU(2)_L \times U(1)_Y \times U(1)_X$. Towards $SO(10)$ unification, we consider an intermediate path with the $SU(5) \times U(1)_X$ unification and show the successful embedding into the $SO(10)$ model with unified gauge couplings. In Sec. III, we describe the system of the extra $U(1)_X$ breaking and discuss the first-order phase transition in the early universe by employing the finite-temperature effective potential for the $U(1)_X$ Higgs field. In Sec. IV, we introduce the formulas that we adopt to compute the GW spectrum generated by the first-order phase transition and present the resultant GW spectrum for various sets of the model parameters. We also discuss the model-parameter dependence of the GW spectrum. The last section is devoted to summary.

¹ Another promising $SO(10)$ breaking path is via Pati-Salam model [53]. GWs could be generated by a low energy Pati-Salam phase transition followed by a late-time inflation to dilute monopoles [54].

II. UV COMPLETION BY $SO(10)$

A. $SO(10) \supset SU(5) \times U(1)_X$ embedding

As previously discussed, we consider the UV completion of the $U(1)$ extended SM by $SO(10)$ GUT via the intermediate step of $SU(5) \times U(1)_X$ unification. To realize this partial unification, we generalize $U(1)_{B-L}$ of the minimal $B-L$ model to $U(1)_X$, under which the charge of an SM field is defined as a linear combination of its hyper-charge and $B-L$ charge, $q_X = Yx + Q_{B-L}$, with x being a real constant [55, 56]. The particle content of this model is listed in Table I. Except for the introduction of new parameter x , the model properties are quite similar to those of the minimal $B-L$ model,² which is realized as the special case of $x = 0$.

	$SU(3)_C$	$SU(2)_L$	$U(1)_Y$	$U(1)_X$
q_L^i	3	2	$\frac{1}{6}$	$\frac{1}{6}x + \frac{1}{3}$
u_R^i	3	1	$\frac{2}{3}$	$\frac{2}{3}x + \frac{1}{3}$
d_R^i	3	1	$-\frac{1}{3}$	$-\frac{1}{3}x + \frac{1}{3}$
l_L^i	1	2	$-\frac{1}{2}$	$-\frac{1}{2}x - 1$
e_R^i	1	1	-1	$-x - 1$
N_R^i	1	1	0	-1
H	1	2	$-\frac{1}{2}$	$-\frac{1}{2}x$
Φ_2	1	1	0	-2

TABLE I: The particle content of the minimal $U(1)_X$ model. In addition to the SM particle content ($i = 1, 2, 3$), three RH neutrinos N_R^i ($i = 1, 2, 3$) and one $U(1)_X$ Higgs field Φ_2 are introduced.

We now consider the embedding,

$$SU(5) \times U(1)_X \supset SU(3)_C \times SU(2)_L \times U(1)_Y \times U(1)_X. \quad (1)$$

As in the standard $SU(5)$ GUT [60], anti right-handed down quarks and left-handed leptons are embedded in $\mathbf{5}^*$ representation of $SU(5)$, while left-handed quarks, anti right-handed up

² See Refs. [57–59] for interesting phenomenology in an extreme case (“hyper-charge oriented” case), namely, $|x| \gg 1$.

quarks, anti right-handed charged leptons are embedded in **10** representation:

$$\mathbf{5}^* \supset d_R^{iC} \oplus \ell_L^i, \quad \mathbf{10} \supset q_L^i \oplus u_R^{iC} \oplus \ell_R^{iC}, \quad (2)$$

This quark and lepton unification requires the following two conditions,

$$\frac{1}{3}x - \frac{1}{3} = -\frac{1}{2}x - 1, \quad \frac{1}{6}x + \frac{1}{3} = -\frac{2}{3}x - \frac{1}{3} = x + 1, \quad (3)$$

which should be satisfied with a unique x value. The solution is $x = -\frac{4}{5}$ and hence the $SU(5)$ unification leads to a quantization of $U(1)_X$ charge [61]. As is well known, the $SU(5)$ GUT normalization for the SM $U(1)_Y$ coupling and rescaled charges are

$$g_Y = \sqrt{\frac{3}{5}}g_1, \quad Q_1 = \sqrt{\frac{3}{5}}Q_Y. \quad (4)$$

The $SU(5) \times U(1)_X$ can be embedded into $SO(10)$. In the following, we list the decomposition of several $SO(10)$ multiplets to $SU(5) \times U(1)_X$ [62]:

$$\begin{aligned} SO(10) &\supset SU(5) \times U(1)_X \\ \mathbf{10} &= \mathbf{5}(-2/5) + \mathbf{5}^*(2/5), \\ \mathbf{16} &= \mathbf{1}(1) + \mathbf{5}^*(-3/5) + \mathbf{10}(1/5), \\ \mathbf{45} &= \mathbf{1}(0) + \mathbf{10}(-4/5) + \mathbf{10}^*(4/5) + \mathbf{24}(0), \\ \mathbf{126} &= \mathbf{1}(2) + \mathbf{5}^*(2/5) + \mathbf{10}(6/5) + \mathbf{15}^*(-6/5) + \mathbf{45}(-2/5) + \mathbf{50}^*(2/5). \end{aligned}$$

The SM fermions and RH neutrinos are embedded in **16** representation. The SM Higgs doublet (H) is embedded in **10** representation,³ while the $U(1)_X$ Higgs field (Φ_2) is in **126** representation. Similarly to the embedding of $U(1)_Y$ into $SU(5)$, the $SO(10)$ GUT normalization of $U(1)_X$ is given by

$$g_X = \sqrt{\frac{5}{8}}g_\chi, \quad Q_\chi = \sqrt{\frac{5}{8}}Q_X. \quad (5)$$

For simplicity, we assume the $SO(10)$ symmetry breaking to the $U(1)_X$ extended SM by non-zero VEVs of $\langle \mathbf{1}(0) \rangle$ and $\langle \mathbf{24}(0) \rangle$ in a **45**-representation Higgs field:

$$SO(10) \xrightarrow{\langle \mathbf{1}(0) \rangle} SU(5) \times U(1)_X \xrightarrow{\langle \mathbf{24}(0) \rangle} SU(3)_C \times SU(2)_L \times U(1)_Y \times U(1)_X. \quad (6)$$

³ In precise, for deriving realistic SM fermion mass matrices, the SM Higgs doublet is identified with a linear combination of $SU(2)_L$ doublets in **10** and **126** representations. See Eq. (7) for the Yukawa coupling in the $SO(10)$ GUT.

The final $U(1)_X$ breaking can be realized by a non-zero VEV of $\Phi_2^\dagger = \mathbf{1}(2) \subset \mathbf{126}$ Higgs field.

In the $SO(10)$ GUT, the Yukawa interactions for the SM fermions are given by

$$\mathcal{L}_{\text{Yukawa}} \supset Y_{10} \mathbf{16}_f \mathbf{16}_f \mathbf{10}_H + Y_{126} \mathbf{16}_f \mathbf{16}_f \mathbf{126}_H^\dagger, \quad (7)$$

where $\mathbf{16}_f$ is a fermion multiplet (the generation index is suppressed), and $\mathbf{10}_H$ and $\mathbf{126}_H$ are Higgs fields. Referring the above decomposition, one can see that the VEV of $\mathbf{1}(2) \subset \mathbf{126}$ Higgs breaks the $U(1)_X$ symmetry and generates Majorana masses of RH neutrinos in $\mathbf{16}_f$ through the Yukawa coupling Y_{126} in Eq. (7). In the SM gauge group decomposition, the Yukawa interactions include the neutrino Dirac Yukawa couplings of $\bar{l}_L H N_R$.

B. Gauge coupling unification to $SU(5)$

	$SU(3)_C$	$SU(2)_L$	$U(1)_Y$	$U(1)_X$
Q	$\mathbf{3}$	$\mathbf{2}$	$\frac{1}{6}$	$\frac{1}{5}$
\bar{Q}	$\mathbf{3}^*$	$\mathbf{2}$	$-\frac{1}{6}$	$-\frac{1}{5}$
D	$\mathbf{3}$	$\mathbf{1}$	$-\frac{1}{3}$	$\frac{3}{5}$
\bar{D}	$\mathbf{3}^*$	$\mathbf{1}$	$\frac{1}{3}$	$-\frac{3}{5}$

TABLE II: Representations of the vector-like quarks.

In non-supersymmetric framework, a simple setup to achieve the unification of the three SM gauge couplings is to introduce two pairs of vector-like quarks ($Q + \bar{Q}$ and $D + \bar{D}$) with TeV scale masses, M_Q and M_D , respectively. Their representations are listed in Table II. It has been shown in Refs. [63–69] that in the presence of the exotic quarks, the SM gauge couplings are successfully unified at $M_{SU(5)} \simeq 10^{16}$ GeV. This unification scale corresponds to the proton lifetime of $\tau_p \simeq 10^{38}$ years, which is much longer than the current experimental lower bound of $\tau(p \rightarrow \pi^0 e^+) \simeq 10^{34}$ years reported by the Super-Kamiokande collaboration [70]. The presence of the exotic quarks can also work for stabilizing the SM Higgs potential [69].

In the $SU(5) \times U(1)_X$ unification, $D + \bar{D}$ are embedded in $(\mathbf{5}, 3/5) + (\mathbf{5}^*, -3/5)$, which are then embedded in $\mathbf{16}^* + \mathbf{16}$ multiplets in the $SO(10)$ GUT. Similarly, $Q + \bar{Q}$ are embedded in $(\mathbf{10}, 1/5) + (\mathbf{10}^*, -1/5)$ and then in $\mathbf{16} + \mathbf{16}^*$ multiplets. To realize a mass splitting which

makes only $D + \bar{D}$ light among the components in the $\mathbf{16}^* + \mathbf{16}$ multiplets, we consider the following Yukawa coupling and mass terms:

$$\begin{aligned} \mathcal{L}_Y &= \mathbf{16}^* (Y \mathbf{45}_H + M) \mathbf{16} \\ &\supset \mathbf{1}^* \left(\sqrt{\frac{5}{8}} Y \mathbf{1}_H + M \right) \mathbf{1} + \mathbf{5}^* \left(-\frac{3}{5} \sqrt{\frac{5}{8}} Y \mathbf{1}_H + Y \mathbf{24}_H + M \right) \mathbf{5} \\ &\quad + \text{tr} \left[\mathbf{10}^* \left(\frac{1}{5} \sqrt{\frac{5}{8}} Y \mathbf{1}_H + Y \mathbf{24}_H + M \right) \mathbf{10} \right], \end{aligned} \quad (8)$$

where $\mathbf{45}_H$ is the $\mathbf{45}$ -representation Higgs field in the $SO(10)$ GUT, and the second and third lines are the expression under $SU(5) \times U(1)_X$. The $SO(10)$ symmetry breaking down to $SU(3)_C \times SU(2)_L \times U(1)_Y \times U(1)_X$ (see Eq. (6)) generates new mass terms, and we have

$$\mathcal{L}_Y \rightarrow M_1 \mathbf{1}^* \mathbf{1} + \mathbf{5}^* (Y \langle \mathbf{24}_H \rangle + M_5) \mathbf{5} + \text{tr} [\mathbf{10}^* (Y \langle \mathbf{24}_H \rangle + M_{10}) \mathbf{10}], \quad (9)$$

with

$$\begin{aligned} M_1 &= \sqrt{\frac{5}{8}} Y \langle \mathbf{1}_H \rangle + M, \\ M_5 &= -\frac{3}{5} \sqrt{\frac{5}{8}} Y \langle \mathbf{1}_H \rangle + M, \\ M_{10} &= \frac{1}{5} \sqrt{\frac{5}{8}} Y \langle \mathbf{1}_H \rangle + M. \end{aligned} \quad (10)$$

We set the parameters, $Y \sim 1$, $\langle \mathbf{1}_H \rangle = \mathcal{O}(M_{SO(10)})$ and $M = \mathcal{O}(M_{SO(10)})$. By tuning them, we can realize $M_5 = \mathcal{O}(M_{SU(5)})$ while $M_1 \sim M_{10} = \mathcal{O}(M_{SO(10)})$. Next, we tune $Y \langle \mathbf{24}_H \rangle \simeq M_5 \text{diag}(-1, -1, -1, 3/2, 3/2)$ so as to make only $D + \bar{D}$ in the $\mathbf{5} + \mathbf{5}^*$ multiplet to be light. This procedure is analogous to the triplet-doublet splitting of the $\mathbf{5}$ -plet Higgs field in the standard $SU(5)$ GUT. We apply the same procedure to the $\mathbf{16} + \mathbf{16}^*$ multiplets including $Q + \bar{Q}$ to leave only them light. This is done by a tuning to realize $M_{10} = \mathcal{O}(M_{SU(5)})$ while $M_1 \sim M_5 = \mathcal{O}(M_{SO(10)})$.

Let us now discuss the gauge coupling unification. At the one-loop level, the renormalization group (GR) equations of the SM gauge couplings and $U(1)_\chi$ gauge couplings are given by

$$\mu \frac{d\alpha_i^{-1}}{d\mu} = -\frac{b_i}{2\pi}, \quad (11)$$

where $\alpha_i = \frac{g_i^2}{4\pi}$ ($i=1, 2, 3$, and χ). The beta function coefficients are expressed as

$$b_i = -\frac{11}{3} C_2(G) + \frac{2}{3} T(R_f) N_{R_f} + \frac{1}{6} T(R_s) N_{R_s}, \quad (12)$$

where $C_2(G)$ is the casimir operator of the group G , $T(R_{f(s)})$ is the trace of the product of generators ($\text{tr}[t^a t^b] = T(R_{f(s)})\delta^{ab}$), and $N_{f(s)}$ is the number of fermions (scalars). For each gauge coupling constant in the energy range of $M_Q, M_D < \mu < M_{\text{SU}(5)}$, we have

$$SU(3)_C : b_3 = b_3^{\text{SM}} + \frac{2}{3}(2+1) = -5, \quad (13)$$

$$SU(2)_L : b_2 = b_2^{\text{SM}} + \frac{2}{3} \times 3 = -\frac{7}{6}, \quad (14)$$

$$U(1)_1 : b_1 = b_1^{\text{SM}} + \frac{3}{5} \times \frac{2}{3} \left(\frac{1}{36} \times 6 \times 2 + \frac{1}{9} \times 3 \times 2 \right) = \frac{9}{2}, \quad (15)$$

$$U(1)_\chi : b_\chi = \frac{5}{8} \times \frac{2}{3} \left\{ \left(\frac{1}{25} \times 6 + \frac{1}{25} \times 3 + \frac{9}{25} \times 3 + \frac{9}{25} \times 2 + \frac{1}{25} \times 1 + 1 \right) \times 3 \right. \\ \left. + 2 \left(\frac{9}{25} \times 3 + \frac{1}{25} \times 6 \right) \right\} + \frac{5}{8} \times \frac{1}{3} \left(\frac{4}{25} \times 2 + 4 \right) = 6, \quad (16)$$

where $b_3^{\text{SM}} = -7$, $b_2^{\text{SM}} = -19/6$ and $b_1^{\text{SM}} = 41/10$ are the beta function coefficients from the SM fields. In the following analysis, we set the vector-like quark masses to be $M_Q = M_D = 1.5$ TeV, which satisfy the latest LHC bounds [71, 72]. One can see that due to the new contributions of the exotic quarks to $b_{2,3}$, the RG evolutions of $g_{2,3}$ are flatten and hence the two gauge couplings merge at a higher energy scale than that in the SM.

In our numerical analysis, we employ the RG equations at the two-loop level (for the beta functions, see, for example, Ref. [68]) and numerically solve the RG equations with the boundary conditions at the top quark pole mass $\mu = M_t = 173.34$ GeV. Adopting the fitting formulas given in Ref. [73], we set $g_1(M_t) = 0.4626$, $g_2(M_t) = 0.6478$, $g_3(M_t) = 1.167$, $y_t(M_t) = 0.9369$, and $\lambda_H(M_t) = 0.2518$, where y_t and λ_H are the running top Yukawa and Higgs quartic couplings, respectively. We find that three SM gauge couplings are successfully unified at $M_{\text{SU}(5)} \simeq 2.24 \times 10^{16}$ GeV. Our results are shown in Fig. 1. We will discuss the RG evolution for g_χ in the next subsection.

C. Gauge coupling unification to $SO(10)$

After the successful unification of the SM gauge group to $SU(5)$ at $M_{\text{SU}(5)}$ we consider the unification of $SU(5) \times U(1)_\chi \rightarrow SO(10)$ at $M_{\text{SO}(10)}$. In the following, let us consider two simple cases: the first is $M_{\text{SU}(5)} = M_{\text{SO}(10)}$, and the second is $M_{\text{SU}(5)} < M_{\text{SO}(10)} = M_P$, where $M_P = 2.43 \times 10^{18}$ GeV is the reduced Planck mass. The first case is very simple, and the running coupling $g_\chi(\mu)$ is determined so as to satisfy the unification condition

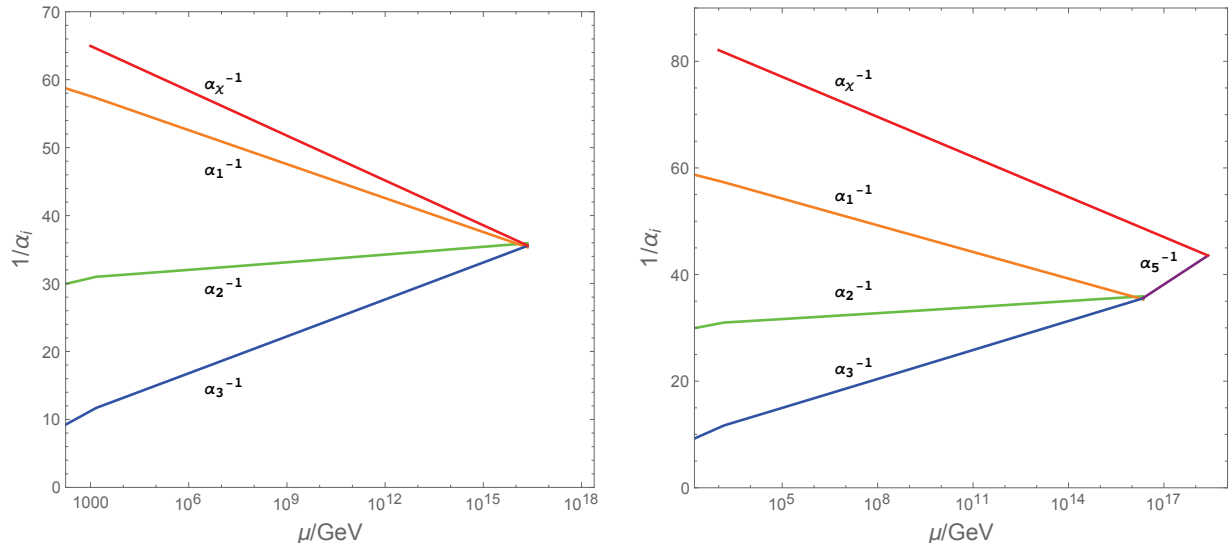


FIG. 1: The RG evolution of the gauge couplings of the $U(1)$ extended SM with the vector-like quarks. Three SM gauge couplings are unified at $M_{\text{SU}(5)} \simeq 2.24 \times 10^{16}$ GeV. *Left panel:* The results for the case of $M_{\text{SU}(5)} = M_{\text{SO}(10)}$. *Right panel:* The results for $M_{\text{SU}(5)} < M_{\text{SO}(10)} = M_P$.

$g_\chi(M_{\text{SU}(5)}) = g_i(M_{\text{SU}(5)})$ ($i = 1, 2, 3$). The result is shown in the left panel of Fig. 1. For the second case, we consider the evolution of the $SU(5)$ gauge coupling g_5 from $M_{\text{SU}(5)}$ to $M_{\text{SO}(10)} = M_P$, and set the boundary condition for g_χ as $g_\chi(M_{\text{SO}(10)}) = g_5(M_{\text{SO}(10)})$.

To calculate the RG evolutions of g_5 and g_χ in the energy range of $M_{\text{SU}(5)} < \mu < M_{\text{SO}(10)}$, we need to know the particle spectrum to determine the beta functions of g_5 and g_χ . We assume the minimal particle content for the $SU(5) \times U(1)$ theory connecting to the particle contents of the $U(1)_X$ extended SM. All the SM fermions and RH neutrinos which are embedded into the three generations of **16**-plets of $SO(10)$ contribute to the beta functions. Under the gauge group $SU(5) \times U(1)_X$, the SM Higgs field is embedded into $(\mathbf{5}, -2/5)$ and the $U(1)_X$ Higgs field is in $(\mathbf{1}, -2)$. In addition, we have an $SU(5)$ adjoint Higgs field with a vanishing $U(1)_X$ charge $(\mathbf{24}, 0)$, whose VEV breaks the $SU(5)$ gauge group to the SM gauge group. Lastly, as we have discussed in Sec. II B, the vector-like quarks, $\bar{Q} + Q$ and $D + \bar{D}$, respectively, are embedded in the full $SU(5)$ multiplets of $\mathbf{10}^* + \mathbf{10}$ and $\mathbf{5} + \mathbf{5}^*$ at $M_{\text{SU}(5)}$. Taking all these fields into account, the beta function coefficient of the $SU(5)$ gauge coupling at the one-loop level is given by

$$b_5 = -\frac{55}{3} + \frac{2}{3} \left(\frac{1}{2} + \frac{3}{2} \right) \times (3 + 2) + \frac{1}{3} \left(\frac{1}{2} + \frac{1}{2} \times 5 \right) = -\frac{32}{3}. \quad (17)$$

The beta function coefficient of the $U(1)_X$ gauge coupling at the one-loop level is given by

$$b_\chi = \frac{5}{8} \left\{ \frac{2}{3} \left(\frac{9}{25} \times 5 + \frac{1}{25} \times 10 \right) \times (3+2) + \frac{2}{3} \times 3 + \frac{1}{3} \left(\frac{4}{25} \times 5 + 4 \right) \right\} = \frac{41}{6}. \quad (18)$$

With these beta function coefficient and the boundary condition $g_5(M_{\text{SO}(10)}) = g_\chi(M_{\text{SO}(10)})$, we find the solutions for the RG equations. Our results are shown in the right panel of Fig. 1.

III. EXTRA $U(1)$ BREAKING

In the low energy effective theory based on $SU(3)_C \times SU(2)_L \times U(1)_Y \times (1)_X$, the Yukawa interactions of N_R are

$$\mathcal{L}_{Yukawa} \supset - \sum_{i=1}^3 \sum_{j=1}^3 Y_D^{ij} \bar{l}_L^i H N_R^j - \frac{1}{2} \sum_{k=1}^3 Y_{N^k} \Phi_2 \overline{N_R^k}^c N_R^k + \text{H.c.}, \quad (19)$$

where the first term is the neutrino Dirac Yukawa coupling, and the second is the Majorana Yukawa couplings. Once the Higgs field Φ_2 develops a nonzero vacuum expectation value (VEV), the $U(1)$ gauge symmetry is broken and the Majorana mass terms of the RH neutrinos are generated. After the electroweak symmetry breaking, tiny neutrino masses are generated through the seesaw mechanism.

In the effective theory, we consider the following tree-level scalar potential:

$$V_0(\Phi_2) = -M_{\Phi_2}^2 \Phi_2 \Phi_2^\dagger + \frac{1}{2} \lambda_2 (\Phi_2 \Phi_2^\dagger)^2. \quad (20)$$

Here, we omit the SM Higgs field (H) part and its interaction terms for not only simplicity but also its little importance in the following discussion, since we are interested in the case that the VEV of the $U(1)_X$ Higgs field is much larger than that of the SM Higgs field.

The $U(1)_X$ Higgs field is expanded around its VEV (v_2) as

$$\Phi_2 = \frac{v_2 + \phi_2 + i\chi_2}{\sqrt{2}}. \quad (21)$$

The scalar masses are expressed as

$$m_{\phi_2}^2 = -M_{\Phi_2}^2 + \frac{3\lambda_2}{2} v_2^2, \quad (22)$$

$$m_{\chi_2}^2 = -M_{\Phi_2}^2 + \frac{\lambda_2}{2} v_2^2. \quad (23)$$

At the classical minimum with $v_2 = \sqrt{2M_{\Phi_2}^2/\lambda_2}$, χ_2 is the would-be Nambu-Goldstone mode eaten by the $U(1)_X$ gauge boson (Z' boson) and $m_{\phi_2}^2 = \lambda_2 v_2^2$. The RH neutrinos N_R^i and the Z' boson acquire their masses as

$$m_{N_R^i} = \frac{Y_{N^i}}{\sqrt{2}} v_2, \quad (24)$$

$$m_{Z'}^2 = q_{\Phi_2}^2 g_X^2 v_2^2. \quad (25)$$

One-loop corrections to the scalar potential for both zero and finite temperatures are essential for realizing the first-order phase transition. One-loop correction is given by

$$\begin{aligned} \Delta V_{1\text{-loop}}(\varphi) = & \sum_s g_s \frac{m_s^4}{64\pi^2} \left(\ln \frac{m_s^2}{Q^2} - c_s \right) - \sum_f g_f \frac{m_f^4}{64\pi^2} \left(\ln \frac{m_f^2}{Q^2} - c_f \right) \\ & + \sum_v g_v \frac{m_v^4}{64\pi^2} \left(\ln \frac{m_v^2}{Q^2} - c_v \right). \end{aligned} \quad (26)$$

Here, g_i , with $i = s$ (scalars), f (fermions) and v (vectors) denotes the number of internal degrees of freedom, $c_i = 5/6$ ($3/2$) are constant for a vector boson (a scalar or a fermion), and Q is the renormalization scale. The finite temperature correction to the effective potential is expressed by

$$\Delta V_T(\varphi) = \sum_s g_s \frac{T^4}{2\pi^2} J_B(m_s^2/T^2) - \sum_f g_f \frac{T^4}{2\pi^2} J_F(m_f^2/T^2) + \sum_v g_v \frac{T^4}{2\pi^2} J_B(m_v^2/T^2), \quad (27)$$

where $J_{B(F)}$ is an auxiliary function in thermal corrections (see e.g., Ref. [74, 75]).

The thermal correction to masses of ϕ_2 , χ_2 and the longitudinal mode of the Z' boson are given by

$$\Delta m_{\phi_2/\chi_2}^2 = \frac{q_{\Phi_2}^2}{4} g_X^2 T^2 + \frac{\lambda_2}{6} T^2 + \sum_N \frac{|Y_N|^2}{24} T^2, \quad (28)$$

$$\Delta m_{Z'_L}^2 = \sum_{\Phi} N_{\Phi} q_{\Phi}^2 \frac{g_X^2}{6} T^2 + \sum_f N_c (q_{L_f}^2 + q_{R_f}^2) \frac{g_X^2}{6} T^2, \quad (29)$$

where q_{Φ} denotes the $U(1)_X$ charge of $\Phi = H, \Phi_2$ respectively, q_L and q_R are those of left- and right-handed fermion f , N_{Φ} is the number of degrees of freedom in Φ , N_c is the color factor, and \sum_f denotes the summation for all fermion flavors. We have the sum of charges

to be

$$\sum_{\Phi} N_{\Phi} q_{\Phi}^2 = 4 \left(\frac{2}{5} \sqrt{\frac{5}{8}} \right)^2 + 2 \left(2 \sqrt{\frac{5}{8}} \right)^2 = \frac{27}{5}, \quad (30)$$

$$\sum_f N_c (q_{L_f}^2 + q_{R_f}^2) = 3 \left\{ (3+2) \left(-\frac{3}{5} \sqrt{\frac{5}{8}} \right)^2 + (2 \times 3 + 3 + 1) \left(\frac{1}{5} \sqrt{\frac{5}{8}} \right)^2 + \left(\sqrt{\frac{5}{8}} \right)^2 \right\} \\ + 3 \left\{ 2 \left(\frac{1}{5} \sqrt{\frac{5}{8}} \right)^2 + 2 \left(-\frac{1}{5} \sqrt{\frac{5}{8}} \right)^2 + \left(\frac{3}{5} \sqrt{\frac{5}{8}} \right)^2 + \left(-\frac{3}{5} \sqrt{\frac{5}{8}} \right)^2 \right\} \quad (31)$$

$$= \frac{153}{20}, \quad (32)$$

where the contribution of the second line in Eq. (31) comes from the vector-like quarks. The thermal masses of the longitudinal mode of the gauge boson as well as the thermal mass of scalars are added and subtracted in the un-resummed Lagrangian, by following to the resummation method [76–78].

For our numerical calculations, we have implemented our model into the public code `CosmoTransitions` [79], where both zero- and finite-temperature one-loop effective potentials with the corrections for resummation,

$$V_{\text{eff}}(\varphi, T) = V_0(\varphi) + \Delta V_{1\text{-loop}}(\varphi) + \Delta V_T(\varphi, T), \quad (33)$$

with $\Phi_2 = \varphi/\sqrt{2}$, have been calculated in the $\overline{\text{MS}}$ renormalization scheme at a renormalization scale $Q^2 = v_2^2$. Here, as a caveat, we note that there is a long-standing open problem of gauge dependence on the use of the effective Higgs potential. Our results are also subjects of this issue [80, 81] and should be regarded as a reference value.

By using `CosmoTransitions`, we calculate the bubble nucleation temperature T_{\star} [82], the latent heat energy density given by

$$\epsilon = \left(V - T \frac{\partial V}{\partial T} \right) \Big|_{\{\phi_{\text{high}}, T_{\star}\}} - \left(V - T \frac{\partial V}{\partial T} \right) \Big|_{\{\phi_{\text{low}}, T_{\star}\}}, \quad (34)$$

where $\phi_{\text{high(low)}}$ denotes the field value of ϕ at the high (low) vacuum and the three-dimensional Euclidean action for the bounce solution of the scalar field in the effective potential (33). We introduce the latent heat to radiation energy density ratio defined by

$$\alpha \equiv \frac{\epsilon}{\rho_{\text{rad}}}. \quad (35)$$

The radiation energy density is given by

$$\rho_{\text{rad}} = \frac{\pi^2 g_*}{30} T^4, \quad (36)$$

with g_* being the total number of relativistic degrees of freedom in the thermal plasma. The bubble nucleation rate per unit volume at a finite temperature is given by

$$\Gamma(T) = \Gamma_0 e^{-S(T)} \simeq \Gamma_0 e^{-S_E^3(T)/T}. \quad (37)$$

Here, Γ_0 is a coefficient of the order of the transition energy scale, S is the action in the four-dimensional Minkowski space, and S_E^3 is the three-dimensional Euclidean action [31].

The transition timescale is characterized by a dimensionless parameter

$$\frac{\beta}{H_*} \simeq T \left. \frac{dS}{dT} \right|_{T_*} = T \left. \frac{d(S_E^3/T)}{dT} \right|_{T_*}, \quad (38)$$

with

$$\beta \equiv - \left. \frac{dS}{dt} \right|_{t_*}. \quad (39)$$

IV. GW SPECTRUM

A. GW generation

There are three mechanisms generating GWs by a first-order phase transition: bubble collisions, sound waves, and turbulence after bubble collisions. The resultant spectrum of GW background produced by each three mechanisms is expressed as

$$\Omega_{GW}(f) = \Omega_{GW}^{\text{coll}}(f) + \Omega_{GW}^{\text{sw}}(f) + \Omega_{GW}^{\text{turb}}(f), \quad (40)$$

in terms of the density parameter Ω_{GW} . Here, three terms in the right hand side denote the GW generated by bubble collisions, sound waves, and turbulence, respectively.

1. Bubble collisions

The GW spectrum generated by bubble collisions for a case of $\beta/H_* \gg 1$ is fitted with

$$\Omega_{GW}^{\text{coll}}(f) = \Omega_{GW}^{\text{coll}}(f_{\text{peak}}) S^{\text{coll}}(f), \quad (41)$$

with the peak amplitude [32]

$$h^2\Omega_{GW}^{\text{coll}}(f_{\text{peak}}) \simeq 1.7 \times 10^{-5} \kappa^2 \Delta \left(\frac{\beta}{H_\star}\right)^{-2} \left(\frac{\alpha}{1+\alpha}\right)^2 \left(\frac{g_\star}{100}\right)^{-1/3}, \quad (42)$$

the peak frequency

$$f_{\text{peak}} \simeq 17 \left(\frac{f_\star}{\beta}\right) \left(\frac{\beta}{H_\star}\right) \left(\frac{T_\star}{10^8 \text{ GeV}}\right) \left(\frac{g_\star}{100}\right)^{1/6} \text{ Hz}, \quad (43)$$

$$\frac{f_\star}{\beta} = \frac{0.62}{1.8 - 0.1v_b + v_b^2}, \quad (44)$$

and the spectral function [82]

$$S^{\text{coll}}(f) = \frac{(a+b)f_{\text{peak}}^b f^a}{bf_{\text{peak}}^{a+b} + af^{a+b}}, \quad (45)$$

$$(a, b) \simeq (2.7, 1.0). \quad (46)$$

The efficiency factor for bubble collisions is given by

$$\kappa = \frac{1}{1+A\alpha} \left(A\alpha + \frac{4}{27} \sqrt{\frac{3\alpha}{2}} \right), \quad (47)$$

with $A = 0.715$ and

$$\Delta = \frac{0.11v_b^3}{0.42 + v_b^2}, \quad (48)$$

denotes the bubble wall velocity v_b dependence [33].

2. Sound waves

The GW spectrum generated by sound waves is fitted by

$$\Omega_{GW}^{\text{sw}}(f) = \Omega_{GW}^{\text{sw}}(f_{\text{peak}}) S^{\text{sw}}(f), \quad (49)$$

with the peak amplitude [38, 39, 83]

$$h^2\Omega_{GW}^{\text{sw}}(f_{\text{peak}}) \simeq 2.7 \times 10^{-6} \kappa_v^2 v_b \left(\frac{\beta}{H_\star}\right)^{-1} \left(\frac{\alpha}{1+\alpha}\right)^2 \left(\frac{g_\star}{100}\right)^{-1/3} (H_\star \tau_{\text{sw}}), \quad (50)$$

The efficiency factor (κ_v) is given by [83]

$$\kappa_v \simeq \begin{cases} v_b^{6/5} \frac{6.9\alpha}{1.36 - 0.037\sqrt{\alpha} + \alpha} & \text{for } v_b \ll c_s \\ \frac{\alpha^{2/5}}{0.017 + (0.997 + \alpha)^{2/5}} & \text{for } v_b \simeq c_s \\ \frac{\alpha}{0.73 + 0.083\sqrt{\alpha} + \alpha} & \text{for } v_b \simeq 1 \end{cases}, \quad (51)$$

with c_s being the sonic speed. In numerical plot shown below, we use the efficiency factor for $v_b \sim 1$ which is realized when friction between wall and fluid is weak [39]. For a given α , there is a variation of a factor in this efficiency factor [83]. This may induce a factor or one order of magnitude difference in the final GW spectrum and does not affect our conclusion qualitatively. The peak frequency [82]

$$f_{\text{peak}} \simeq 19 \frac{1}{v_b} \left(\frac{\beta}{H_\star} \right) \left(\frac{T_\star}{10^8 \text{ GeV}} \right) \left(\frac{g_\star}{100} \right)^{1/6} \text{ Hz}, \quad (52)$$

and the spectral function [84]

$$S^{\text{sw}}(f) = \left(\frac{f}{f_{\text{peak}}} \right)^3 \left(\frac{7}{4 + 3 \left(\frac{f}{f_{\text{peak}}} \right)^2} \right)^{7/2}. \quad (53)$$

The active period of sound waves is expressed as

$$\tau_{\text{sw}} = \frac{R_\star}{U_f}, \quad (54)$$

where $R_\star \simeq (8\pi)^{1/3} v_b / \beta$ is the average separation of between bubbles and U_f is the root-mean square of fluid velocity, which can be approximated as [39]

$$U_f^2 \simeq \frac{3}{4} \left(\frac{\alpha}{1 + \alpha} \right) \kappa_v. \quad (55)$$

The last factor in Eq. (50) represents the suppression effect due to the short-lasting sonic wave as a source of gravitational wave generation compared with the Hubble time scale (H_\star) for the case of $H_\star \tau_{\text{sw}} < 1$, as pointed out in Refs. [85, 86] (see also Refs. [87–90]).

3. Turbulence

The GW spectrum generated by turbulence is fitted by

$$\Omega_{GW}^{\text{turb}}(f) = \Omega_{GW}^{\text{turb}}(f_{\text{peak}}) S^{\text{turb}}(f), \quad (56)$$

with the peak amplitude [33]

$$h^2 \Omega_{GW}^{\text{turb}}(f_{\text{peak}}) \simeq 3.4 \times 10^{-4} v_b \left(\frac{\beta}{H_\star} \right)^{-1} \left(\frac{\kappa_{\text{turb}} \alpha}{1 + \alpha} \right)^{3/2} \left(\frac{g_\star}{100} \right)^{-1/3}, \quad (57)$$

the peak frequency

$$f_{\text{peak}} \simeq 27 \frac{1}{v_b} \left(\frac{\beta}{H_\star} \right) \left(\frac{T_\star}{10^8 \text{ GeV}} \right) \left(\frac{g_\star}{100} \right)^{1/6} \text{ Hz}, \quad (58)$$

g_χ	$Q(=v_2)$	$\Delta\rho/(0.1Q)^4$	$T_*/(0.1Q)$	Action	α	β/H_*
0.447	10 TeV	12.8381	0.8865	125.9341	0.6318	341.74
0.455	10^2 TeV	12.8277	0.8728	116.0031	0.6719	343.69
0.463	10^3 TeV	12.8105	0.8573	106.1279	0.7209	299.61
0.473	10^4 TeV	12.7969	0.8426	96.6074	0.7717	259.75
0.482	10^5 TeV	12.7719	0.8247	87.0567	0.8393	242.64

TABLE III: Input and output parameters for the several benchmark points are listed. In our calculations, we have set $\lambda_2 = 6 \times 10^{-4}$.

and the spectral function [37, 84, 91]

$$S^{\text{turb}}(f) = \frac{\left(\frac{f}{f_{\text{peak}}}\right)^3}{\left(1 + \frac{f}{f_{\text{peak}}}\right)^{11/3} \left(1 + \frac{8\pi f}{h_*}\right)}, \quad (59)$$

$$h_* = 17 \left(\frac{T_*}{10^8 \text{GeV}}\right) \left(\frac{g_*}{100}\right)^{1/6} \text{Hz}. \quad (60)$$

We set the efficiency factor for turbulence to be $\kappa_{\text{turb}} \simeq 0.05\kappa_v$.

B. Predicted spectrum for benchmark points

At first, we show the dependence of the resultant GW spectrum on the energy scale of symmetry breaking, or equivalently, the VEV (v_2) scale. In Fig. 2 we show the GW spectrum for various symmetry breaking scales for a fixed value of $\lambda_2 = 6 \times 10^{-4}$. As is expected, the peak frequency becomes higher, as a symmetry breaking occurs at higher energies. The black solid curves denote the expected sensitivities of each indicated experiments: LISA, DECIGO, BBO, Einstein Telescope (ET), and Cosmic Explore (CE). Expected sensitivity curves for each experiments are quoted from Ref. [92]. We list our results for five benchmark points in Table III.

Next, we study how the $U(1)_X$ Higgs quartic coupling and Yukawa coupling affect the resultant GW spectrum. In Ref. [23], it has been shown in the context of the minimal $U(1)_{B-L}$ model that the peak amplitude decreases with the peak frequency getting higher as λ_2 increases, and this dependence is approximated as $\Omega_{\text{GW}} h^2(f_{\text{peak}}) \propto \lambda_2^{-1/4}$ and $f_{\text{peak}} \propto \lambda_2$. As λ_2 increases, the tree level potential (20) becomes more significant. The negative mass

Y_N	λ_2	$\Delta\rho/(0.1Q)^4$	$T_*/(0.1Q)$	Action	α	β/H_*
0.	0.002	17.1290	1.3725	167.3686	0.1467	477.46
0.	0.006	33.0336	2.1506	258.5560	0.0469	821.17
1.	0.001	2.2088	0.7537	93.5851	0.2080	892.03
1.	0.002	4.0694	0.9977	122.9623	0.1248	1034.35
1.	0.006	15.2125	1.6639	201.6852	0.0603	1406.19

TABLE IV: Input and output parameters of several benchmark points varying λ_2 and y_N are listed. We have set $g_\chi = 0.463$ and $v_2 = 1$ PeV in this calculation.

squared at the field origin becomes sizable and the potential becomes steeper as a whole. Then, the strength of the first order phase transition becomes weaker and α becomes smaller. Thus, the amplitude of GW decreases. We do not only reconfirm this λ_2 dependence in the $SO(10)$ completed model but also find that non-vanishing Yukawa coupling has a similar effect on the GW spectrum. As a Yukawa coupling increases, the peak amplitude decreases with the peak frequency increasing. This is because fermion loops generate only thermal mass term but do not an effective trilinear term in thermal potential (27), which weakens the first order phase transition. Assuming the hierarchy among the Yukawa couplings as $Y_{N_3} \equiv Y_N \gg Y_{N_2}, Y_{N_1}$, for simplicity, we show in Fig. 3 the GWs spectrum for various values of Y_N and λ_2 for $g_\chi = 0.463$ and $v_2 = 1$ PeV (see the third benchmark in Table III). In the figure, we see that two different parameter sets, $(Y_N, \lambda_2) = (0, 0.002)$ and $(Y_N, \lambda_2) = (1, 0.001)$, predict almost the same GW spectrum. This is because the dependence of the resultant GW spectrum on Y_N is quite similar to that of λ_2 . We have found that for $\lambda_2 \gtrsim 0.006$, the dependence of GW spectrum on Y_N is weak. We list our results for five benchmark points in Table IV.

V. SUMMARY

In this paper, we have considered the $U(1)_X$ extended SM and studied the spectrum of stochastic GWs generated by the first-order phase transition associated with the extra $U(1)_X$ symmetry breaking in the early universe. This breaking is responsible for the generation of Majorana masses of RH neutrinos. We have investigated a UV completion of the $U(1)_X$

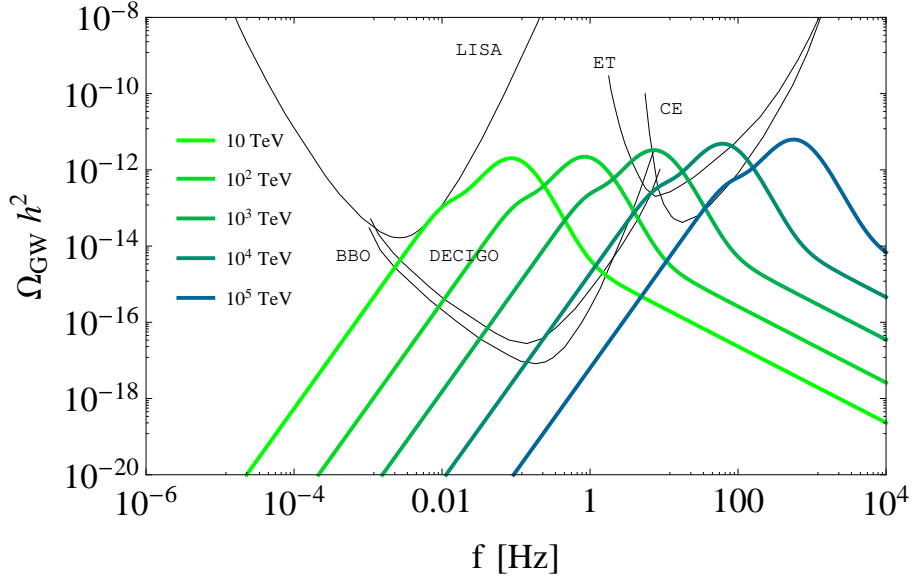


FIG. 2: The predicted GW spectrum for various symmetry breaking scales for $\lambda_2 = 6 \times 10^{-4}$. The difference of the symmetry breaking scale is indicated by colors as shown in legends. Black solid curves are the expected sensitivities of each indicated experiments derived in Ref. [92].

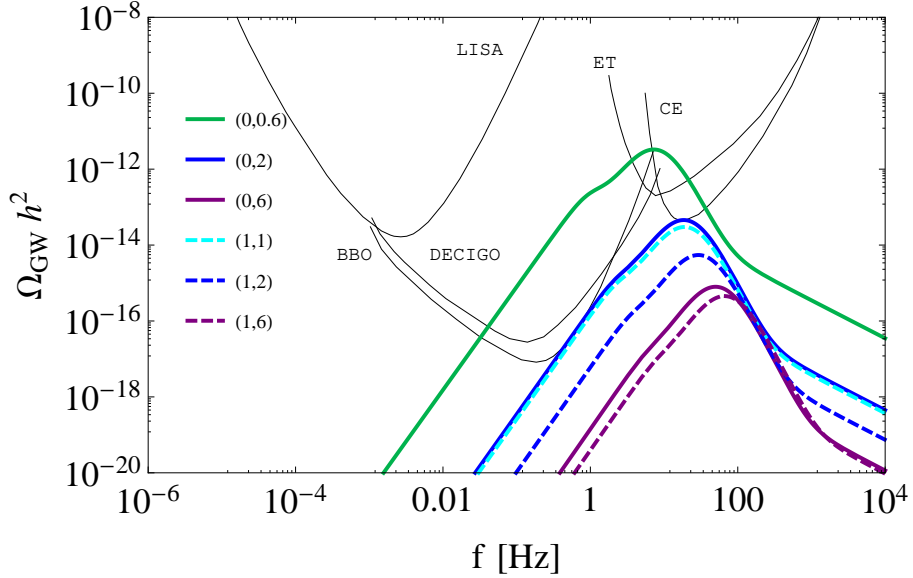


FIG. 3: The predicted GW spectrum for various values of Y_N and λ_2 for $g_\chi = 0.463$ and $v_2 = 1$ PeV. Parameters in the legend denote $(Y_N, \lambda_2 \times 10^3)$.

extended SM by an $SO(10)$ GUT. In this UV completion, the extra $U(1)$ gauge coupling is unified with the SM gauge couplings and thus the extra $U(1)$ gauge coupling at the phase transition epoch is no longer a free parameter and $g_\chi \sim 0.4$ from the gauge coupling unification condition. We have found that the first-order phase transition triggered by this extra $U(1)$ symmetry breaking can be strong enough to generate GWs with a detectable size of amplitude if the $U(1)_X$ Higgs quartic coupling is small enough and the symmetry breaking scale (the bubble nucleation temperature T_*) is smaller than about 10^5 (10^4) PeV.

We have also clarified the dependence of the resultant GW spectrum on the RH neutrino Majorana Yukawa couplings, in other words, the mass scale of RH neutrinos. As the Yukawa couplings increase, the amplitude of GW background reduces and the peak frequency slightly increases. We have found a similar behavior of the GW spectrum as we change the $U(1)_X$ Higgs quartic coupling. Thus, different combinations of the Yukawa and the quartic couplings can result in almost the same GW spectrum. In order to extract the information about RH neutrino masses from the spectral shape of GW background, the information of the $U(1)_X$ Higgs quartic coupling is necessary.

Acknowledgments

This work is supported in part by the U.S. DOE Grant No. DE-SC0012447 (N.O.), the Japan Society for the Promotion of Science (JSPS) KAKENHI Grants No. 19K03860 and No. 19H05091 and No. 19K03865 (O.S.), and the JSPS Research Fellowships for Young Scientists, No. 20J20388 (H.U.).

-
- [1] J. C. Pati and A. Salam, Phys. Rev. D **8**, 1240-1251 (1973).
 - [2] A. Davidson, Phys. Rev. D **20**, 776 (1979).
 - [3] R. N. Mohapatra and R. E. Marshak, Phys. Rev. Lett. **44**, 1316 (1980) [Erratum-ibid. **44**, 1643 (1980)].
 - [4] R. E. Marshak and R. N. Mohapatra, Phys. Lett. B **91**, 222 (1980).
 - [5] P. Minkowski, Phys. Lett. **67B**, 421 (1977).
 - [6] T. Yanagida, Conf. Proc. C **7902131**, 95 (1979).
 - [7] M. Gell-Mann, P. Ramond, and R. Slansky, Conf. Proc. C **790927**, 315 (1979).

- [8] R. N. Mohapatra and G. Senjanovic, Phys. Rev. Lett. **44**, 912 (1980).
- [9] S. Khalil and O. Seto, JCAP **0810**, 024 (2008).
- [10] N. Okada and O. Seto, Phys. Rev. D **82**, 023507 (2010).
- [11] N. Okada and S. Okada, Phys. Rev. D **93**, 075003 (2016).
- [12] N. Okada and S. Okada, Phys. Rev. D **95**, 035025 (2017).
- [13] N. Okada and O. Seto, Mod. Phys. Lett. A **33**, 1850157 (2018).
- [14] S. Okada, Adv. High Energy Phys. **2018**, 5340935 (2018).
- [15] R. Jinno, K. Nakayama and M. Takimoto, Phys. Rev. D **93**, 045024 (2016).
- [16] R. Jinno and M. Takimoto, Phys. Rev. D **95**, 015020 (2017).
- [17] W. Chao, W. F. Cui, H. K. Guo and J. Shu, arXiv:1707.09759 [hep-ph].
- [18] K. Hashino, M. Kakizaki, S. Kanemura, P. Ko and T. Matsui, JHEP **1806**, 088 (2018).
- [19] N. Okada and O. Seto, Phys. Rev. D **98**, 063532 (2018).
- [20] K. Hashino, R. Jinno, M. Kakizaki, S. Kanemura, T. Takahashi and M. Takimoto, Phys. Rev. D **99**, no. 7, 075011 (2019).
- [21] V. Brdar, A. J. Helmboldt and J. Kubo, JCAP **1902**, 021 (2019).
- [22] C. Marzo, L. Marzola and V. Vaskonen, Eur. Phys. J. C **79**, no. 7, 601 (2019).
- [23] T. Hasegawa, N. Okada and O. Seto, Phys. Rev. D **99**, no. 9, 095039 (2019).
- [24] N. Haba and T. Yamada, Phys. Rev. D **101**, no.7, 075027 (2020).
- [25] C. Caprini and D. G. Figueroa, Class. Quant. Grav. **35**, 163001 (2018).
- [26] A. Mazumdar and G. White, Rept. Prog. Phys. **82**, no. 7, 076901 (2019).
- [27] C. Caprini, M. Chala, G. C. Dorsch, M. Hindmarsh, S. J. Huber, T. Konstandin, J. Kozaczuk, G. Nardini, J. M. No, K. Rummukainen, P. Schwaller, G. Servant, A. Tranberg and D. J. Weir, JCAP **03**, 024 (2020).
- [28] M. S. Turner and F. Wilczek, Phys. Rev. Lett. **65**, 3080 (1990).
- [29] A. Kosowsky, M. S. Turner and R. Watkins, Phys. Rev. D **45**, 4514 (1992).
- [30] A. Kosowsky, M. S. Turner and R. Watkins, Phys. Rev. Lett. **69**, 2026 (1992).
- [31] M. S. Turner, E. J. Weinberg and L. M. Widrow, Phys. Rev. D **46**, 2384 (1992).
- [32] A. Kosowsky and M. S. Turner, Phys. Rev. D **47**, 4372 (1993).
- [33] M. Kamionkowski, A. Kosowsky and M. S. Turner, Phys. Rev. D **49**, 2837 (1994).
- [34] A. Kosowsky, A. Mack and T. Kahniashvili, Phys. Rev. D **66**, 024030 (2002).
- [35] A. D. Dolgov, D. Grasso and A. Nicolis, Phys. Rev. D **66**, 103505 (2002).

- [36] G. Gogoberidze, T. Kahniashvili and A. Kosowsky, *Phys. Rev. D* **76**, 083002 (2007).
- [37] C. Caprini, R. Durrer and G. Servant, *JCAP* **0912**, 024 (2009).
- [38] M. Hindmarsh, S. J. Huber, K. Rummukainen and D. J. Weir, *Phys. Rev. Lett.* **112**, 041301 (2014).
- [39] M. Hindmarsh, S. J. Huber, K. Rummukainen and D. J. Weir, *Phys. Rev. D* **92**, 123009 (2015).
- [40] M. Hindmarsh, *Phys. Rev. Lett.* **120**, 071301 (2018).
- [41] G. M. Harry, P. Fritschel, D. A. Shaddock, W. Folkner and E. S. Phinney, *Class. Quant. Grav.* **23**, 4887 (2006); Erratum: [*Class. Quant. Grav.* **23**, 7361 (2006)].
- [42] N. Seto, S. Kawamura and T. Nakamura, *Phys. Rev. Lett.* **87**, 221103 (2001).
- [43] G. M. Harry [LIGO Scientific Collaboration], *Class. Quant. Grav.* **27**, 084006 (2010).
- [44] M. Punturo *et al.*, *Class. Quant. Grav.* **27**, 194002 (2010).
- [45] See, for example, T. Fukuyama, *Int. J. Mod. Phys. A* **28**, 1330008 (2013), references therein.
- [46] J. A. Dror, T. Hiramatsu, K. Kohri, H. Murayama and G. White, *Phys. Rev. Lett.* **124**, no.4, 041804 (2020).
- [47] W. Buchmuller, V. Domcke, H. Murayama and K. Schmitz, [arXiv:1912.03695 [hep-ph]].
- [48] S. Blasi, V. Brdar and K. Schmitz, [arXiv:2004.02889 [hep-ph]].
- [49] S. F. King, S. Pascoli, J. Turner and Y. L. Zhou, arXiv:2005.13549 [hep-ph].
- [50] C. Grojean and G. Servant, *Phys. Rev. D* **75**, 043507 (2007).
- [51] P. S. B. Dev and A. Mazumdar, *Phys. Rev. D* **93**, 104001 (2016).
- [52] C. Balazs, A. Fowlie, A. Mazumdar and G. White, *Phys. Rev. D* **95**, 043505 (2017).
- [53] J. C. Pati and A. Salam, *Phys. Rev. D* **10**, 275-289 (1974).
- [54] D. Croon, T. E. Gonzalo and G. White, *JHEP* **02**, 083 (2019).
- [55] T. Appelquist, B. A. Dobrescu and A. R. Hopper, *Phys. Rev. D* **68** 035012 (2003).
- [56] S. Oda, N. Okada and D. s. Takahashi, *Phys. Rev. D* **92**, no. 1, 015026 (2015).
- [57] N. Okada, S. Okada and D. Raut, *Phys. Rev. D* **95** no.5, 055030 (2017).
- [58] S. Oda, N. Okada, D. Raut and D. s. Takahashi, *Phys. Rev. D* **97** no.5, 055001 (2018).
- [59] N. Okada, S. Okada and Q. Shafi, [arXiv:2003.02667 [hep-ph]].
- [60] H. Georgi and S. L. Glashow, *Phys. Rev. Lett.* **32**, 438 (1974).
- [61] N. Okada, S. Okada and D. Raut, *Phys. Lett. B* **780**, 422 (2018).
- [62] R. Slansky, *Phys. Rept.* **79**, 1 (1981).

- [63] U. Amaldi, W. de Boer, P. H. Frampton, H. Furstenau and J. T. Liu, Phys. Lett. B **281**, 374 (1992).
- [64] J. L. Chkareuli, I. G. Gogoladze and A. B. Kobakhidze, Phys. Lett. B **340**, 63 (1994).
- [65] J. L. Chkareuli, I. G. Gogoladze and A. B. Kobakhidze, Phys. Lett. B **376**, 111 (1996).
- [66] D. Choudhury, T. M. P. Tait and C. E. M. Wagner, Phys. Rev. D **65**, 053002 (2002).
- [67] D. E. Morrissey and C. E. M. Wagner, Phys. Rev. D **69**, 053001 (2004).
- [68] I. Gogoladze, B. He and Q. Shafi, Phys. Lett. B **690**, 495 (2010).
- [69] H. Y. Chen, I. Gogoladze, S. Hu, T. Li and L. Wu, Eur. Phys. J. C **78**, no. 1, 26 (2018).
- [70] K. Abe *et al.* [Super-Kamiokande Collaboration], Phys. Rev. D **95**, no. 1, 012004 (2017).
- [71] A. M. Sirunyan *et al.* [CMS Collaboration], JHEP **1808**, 177 (2018).
- [72] A. M. Sirunyan *et al.* [CMS Collaboration], Phys. Rev. D **100**, no. 7, 072001 (2019).
- [73] D. Buttazzo, G. Degrossi, P. P. Giardino, G. F. Giudice, F. Sala, A. Salvio and A. Strumia, JHEP **1312**, 089 (2013).
- [74] M. L. Bellac, *Thermal Field Theory*, Cambridge University Press (1996).
- [75] J. I. Kapusta and C. Gale, *Finite-Temperature Field Theory: Principles and Applications*, Cambridge University Press (2011).
- [76] M. E. Carrington, Phys. Rev. D **45**, 2933-2944 (1992).
- [77] R. R. Parwani, Phys. Rev. D **45**, 4695 (1992).
- [78] K. Funakubo and E. Senaha, Phys. Rev. D **87**, no.5, 054003 (2013).
- [79] C. L. Wainwright, Comput. Phys. Commun. **183**, 2006 (2012).
- [80] C. L. Wainwright, S. Profumo and M. J. Ramsey-Musolf, Phys. Rev. D **86**, 083537 (2012).
- [81] C. W. Chiang and E. Senaha, Phys. Lett. B **774**, 489 (2017).
- [82] S. J. Huber and T. Konstandin, JCAP **0809**, 022 (2008).
- [83] J. R. Espinosa, T. Konstandin, J. M. No and G. Servant, JCAP **1006**, 028 (2010).
- [84] C. Caprini *et al.*, JCAP **1604**, no. 04, 001 (2016).
- [85] J. Ellis, M. Lewicki and J. M. No, JCAP **1904**, 003 (2019).
- [86] J. Ellis, M. Lewicki, J. M. No and V. Vaskonen, JCAP **1906**, 024 (2019).
- [87] D. Cutting, M. Hindmarsh and D. J. Weir, Phys. Rev. Lett. **125**, no.2, 021302 (2020).
- [88] M. Hindmarsh and M. Hijazi, JCAP **1912**, no. 12, 062 (2019).
- [89] J. Ellis, M. Lewicki and J. M. No, JCAP **07**, 050 (2020)
- [90] K. Schmitz, [arXiv:2005.10789 [hep-ph]].

- [91] P. Binetruy, A. Bohe, C. Caprini and J. F. Dufaux, JCAP **1206**, 027 (2012).
- [92] K. Schmitz, arXiv:2002.04615 [hep-ph].